Notice of Violation of IEEE Publication Principles

"Analysis of Cerebral Blood Flow Imaging by Registered Laser Speckle Contrast Analysis (rLASCA)"
by M.S. Sini, J. Arul Linsely
in the Proceedings of the International Conference on Signal Processing, Communication, Computing and Networking Technologies (ICSCCN), 2011, pp. 207-212

After careful and considered review of the content and authorship of this paper by a duly constituted expert committee, this paper has been found to be in violation of IEEE's Publication Principles.

This paper is a duplication of the original text from the paper cited below. The original text was copied without attribution (including appropriate references to the original author(s) and/or paper title) and without permission.

Due to the nature of this violation, reasonable effort should be made to remove all past references to this paper, and future references should be made to the following article:

"High Resolution Cerebral Blood Flow Imaging by Registered Laser Speckle Contrast Analysis"
by Peng Miao, Abhishek Rege, Nan Li, Nitish V. Thakor, and Shanbao Tong
in the IEEE Transactions on Biomedical Engineering, Vol 57, No 5, May 2010, pp. 1152-1157

Analysis of Cerebral Blood Flow Imaging by Registered Laser Speckle Contrast Analysis (rLASCA)

M.S.Sini,
Student: Dept of EEE ,
Noorul Islam University, Kumaracoil,
Thuckalay, Kanyakumari district, India.
sini87mohan@gmail.com,mohan_sini@yahoo.com.

Prof .J .Arul Linsely,
Lecturer: Dept of EEE,
Noorul Islam University, Kumaracoil,
Thuckalay, Kanyakumari district, India.
arul_linsely@yahoo.com

***Abstract*—Laser speckle imaging (LSI) has been widely used for *in vivo* detecting cerebral blood flow (CBF) under various physiological and pathological conditions. So far, nearly all literature on *in vivo* LSI does not consider the influence of disturbances due to respiration and/or heart beating of animals. In this paper, we analyze how such physiologic motions affect the spatial resolution of the conventional laser speckle contrast analysis (LASCA).We propose a registered laser speckle contrast analysis (rLASCA) method which first registers raw speckle images with a 3×3 convolution kernel, normalized correlation metric and cubic B-spline interpolator, and then constructs the contrast image for CBF. rLASCA not only significantly improves the distinguishability of small vessels, but also efficiently suppresses the noises induced by respiration and/or heart beating. In an application of imaging the angiogenesis of rat's brain tumor, rLASCA outperformed the conventional LASCA in providing a much higher resolution for new small vessels. As a processing method for LSI, rLASCA can be directly applied to other LSI experiments where the disturbances from different sources (like respiration, heart beating) exist.**

***Index Terms*—Cubic B-spline interpolation, laser speckle imaging (LSI), normalized correlation registration, registered laser speckle contrast analysis (rLASCA).**

I. INTRODUCTION

AS a 2-D and non invasive optical imaging technique, laser speckle imaging (LSI) has been widely used to study rat's cerebral blood flow (CBF) under a variety of physiological and pathological conditions, e.g., focal cerebral ischemia, hypotension, peripheral electrical stimulation , hypothermia , and brain tumor . When the tissue contains scattering moving particles, e.g., blood cells, sequentially recorded raw speckle images $\{I_i(x, y)\}(i = 1, \ldots, N)$ are analyzed by laser speckle contrast analysis (LASCA) to obtain both CBF and vessel structure information. According to the theory of LASCA, the contrast value K^2 , defined as the square of ratio of standard deviation σ to mean intensity <I>, is inversely proportional to velocity *v*. K^2 can be estimated in either spatial or temporal K^2_t) formalism. For each frame of the

$$K^2 = \frac{\sigma}{<I>} \propto \frac{1}{V} \quad (1)$$

acquired Speckle images, K_s for each pixel is calculated based on the intensities in a small window (typically 7×7), and therefore loses the spatial resolution. Similarly, K^2_t at each pixel is estimated using the intensities of the pixel in continuously recorded raw speckle images. In practice, 50 or more frames are used for statistical efficiency. As a result, K^2_t retains the spatial resolution but temporal resolution is compromised.

Like other optical imaging techniques, LSI is also susceptible to kinds of mechanical vibrations within the workspace. Such mechanical vibrations can be minimized by using vibration isolated optical platform and other precautions. In rodent *in vivo* experiments, the animals are always anesthetized and constrained in a stereo taxic frame to suppress movements. However, there are still some inevitable disturbances in raw speckle images due to respiration and/or heart beating of the animals. Such global disturbances could lead to the following problems in LASCA:

1) The loss of spatial resolution, the output of LASCA is going to be blurred, and thus it is more difficult to distinguish small vessels from tissue;

2) Inaccurate estimation of contrast values, disturbances change the statistic property of the speckles and lead to inaccurate estimation of CBF by LASCA. In order to overcome these problems, we propose to register the raw speckle images before LASCA, or called registered LASCA (rLASCA) hereafter. Since the raw speckle images are usually too noisy to find a stable pattern for registration, we develop a novel automatic registration technique, using a 3×3 convolution kernel, a normalized correlation metric and a cubic B-spline interpolator, to register raw speckle images accurately. rLASCA is shown to enhance the small vessels and alleviate noises in both tissue area and vessels. As an application, we studied the angiogenesis in rat's brain tumor by LSI, and showed how rLASCA improves the resolution of cortical vascular structure of the angiogenesis.

978-1-61284-653-8/11/$26.00 ©2011 IEEE

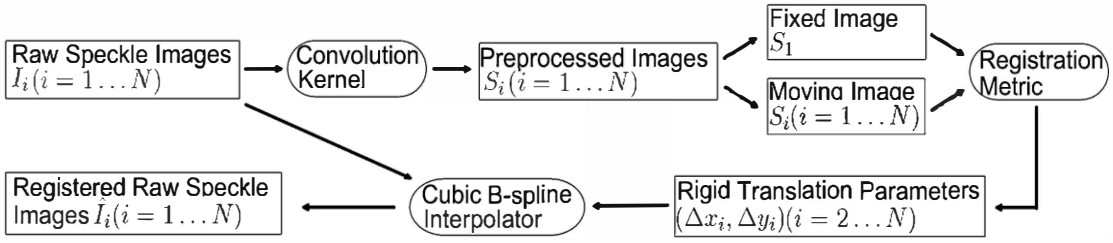

Fig. 1. Registration procedure based on the modified registration method

II. METHOD

rLASCA involves two steps: 1) registering raw speckle images $\{I_i(x, y)\}(i = 1, \ldots, N)$ and

2) Calculating LASCA based on the registered raw speckle images $\{\hat{I}_i(x, y)\}(i = 1, \ldots, N)$.

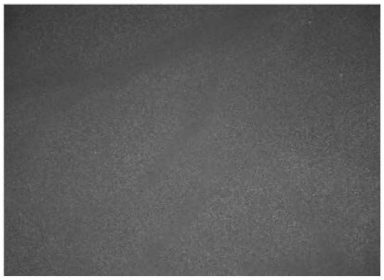

Fig. 2. One raw speckle image.

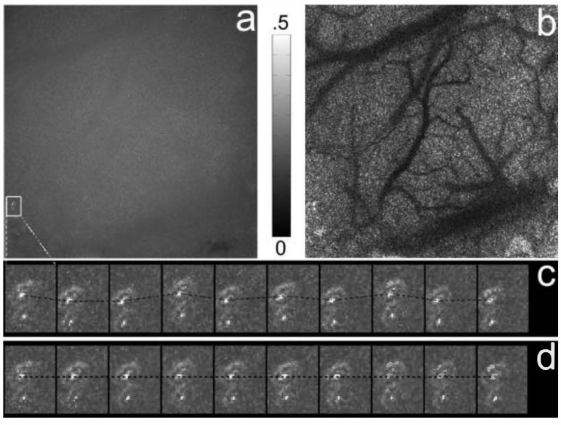

Fig. 3. (a) One typical raw speckle image. (b) Preprocessed image of (a) using a 3×3 convolution kernel. (c) Zoomed out images of white box area in first ten frames with obvious disturbances. (d) Images of the same area after registration with eliminated disturbances.

A. Registering Raw Speckle Images by Modified Registration Technique

Traditional registration techniques are incapable of processing raw speckle images $\{I_i(x, y)\}$ $(i = 1, \ldots, N)$, because the random speckles indicate no stable pattern, which could be used for registration [see Fig. 3(a)]. Occasionally, there are some isolated pixels overexposed due to strong reflection [e.g., white boxed area in Fig. 3(a)], in which case, the continuously acquired speckle images can be registered based on these overexposed pixels. However, in practice, the existence of such overexposed area is neither guaranteed nor desired. In this paper, we propose a novel registration technique to register the raw speckle images. First, each raw speckle image $I_i(x, y)(i = 1, \ldots, N)$ is preprocessed by a 3×3 convolution kernel as described in the following to reveal vessel structure pattern. Then a rigid translation parameter $(\Delta x_i, \Delta y_i)$ is estimated for each preprocessed image $S_i(x, y)$ $(i = 1, \ldots, N)$ by a normalized correlation metric. Finally, the raw speckle images $\{I_i(x, y)\}(i = 1, \ldots, N)$ are registered (resampled) by a cubic B-spline interpolator based on their rigid translation parameters $(\Delta x_i, \Delta y_i)$ to obtain the registered raw speckle images $\{\hat{I}_i(x, y)\}$ $(i = 1, \ldots, N)$.

1) Preprocessing with 3×3 Convolution Kernel:

A 3×3 convolution kernel (2) is implemented to preprocess each raw speckle image to obtain the spatial standard deviation at each pixel, which is related to vessel structure information (3)

$$kernel = \begin{pmatrix} 1 & 1 & 1 \\ 1 & 1 & 1 \\ 1 & 1 & 1 \end{pmatrix} \qquad (2)$$

$$S_i^2 = (I_i^2 \otimes \text{Kernel}) - (I_i \otimes \text{Kernel})^2 \qquad (3)$$

Here for a given matrix A with pixel index (x, y), A^2 represents $A^2(x, y) = (A(x, y))^2$.

Based on (3), the size of image S_i is equal to that of I_i. Since the convolution kernel size is 3×3, only the information at the four borders (the first row, the first column, the last row, and the last column) of S_i is lost. Therefore, the average loss of spatial resolution in this preprocessing step is very small and always less than one pixel

preprocessed images [see Fig. 3(b)], i.e., $S_i(x, y)(i = 1, \ldots, N)$, reveal the same vessel structure pattern which, therefore, can be used for registering $\{I_i(x, y)\}(i = 1, \ldots, N)$ with a minor loss of spatial resolution

.

2) Obtaining Rigid Translation Parameters Based on Normalized Correlation Metric:

In this step, each image $S_i(i = 2, \ldots, N)$ is to be registered to the first image S_1 in accordance with a proper rigid translation. The optimized rigid translation parameter $(\Delta x_i, \Delta y_i)$ for each $S_i(i = 2, \ldots, N)$ is determined by maximizing the normalized correlation metric (4) using a gradient descent optimization procedure with a variable step length

$$Metric = \frac{\sum_{x,y} S_1(x,y) S_i(x - \Delta x_i, y - \Delta y_i)}{\sqrt{\sum_{x,y} S_1^2(x.y) \sum_{x,y} S_i^2(x - \Delta x_i, y - \Delta y_i)}} \quad \ldots. \quad (4)$$

Among various registration metrics, we have chosen the normalized correlation metric for its advantages of low computational cost and well-defined maxima (sharp peaks) in the cost function. All rigid translation parameters $(\Delta x_i, \Delta y_i)$ are used to register (resample) the corresponding raw speckle images $\{I_i(x, y)\}(i = 1, \ldots, N)$ in the next step.

3) Resampling Raw Speckle Images Using Cubic B-Spline Interpolator:

The displacement due to disturbances need not conform to integral pixels, so the rigid translation parameters $(\Delta x_i, \Delta y_i)$ always have subpixel precision. Therefore, a resampling interpolation is needed to register the raw speckle images $\{I_i(x, y)\}$ $(i = 1. . . N)$.

In this study, the cubic B-spline interpolator is used to calculate the intensity of nongrid position in a two dimensional piecewise polynomial way based on the cubic B-spline function (5) which is smooth, continuous and bounded

$$\beta^3(d) = \begin{cases} \frac{2}{3} - |d|^2(2 - |d|)/2, & 0 \le |d| < 1 \\ \frac{2-|d|^3}{6}, & 1 \le |d| < 2 \\ o, & 2 \le |d| \end{cases} \quad (5)$$

where $|d|$ is the distance from the interpolated point.

Although the computational cost of B-spline interpolation is not very low, it is used in this study because cubic B-spline interpolation utilizes the non-integer parameters which is preferable over the nearest neighbour interpolation . In addition, cubic B-spline interpolation prevents the effect of degeneration in linear interpolation.

After resampling, the registered raw speckle images $\hat{I}_i(i = 1, \ldots, N)$ are obtained. The above registration procedures are summarized in Fig.1.

B. Temporal LASCA Based on Registered Speckle Images

After registration as described earlier, the registered raw speckle images $\hat{I}_i(i = 1, \ldots, N)$ are then analyzed by conventional temporal LASCA to obtain maps of blood vessels and flow. The whole procedure as described earlier is then called registered LASCA (rLASCA)

III. Experiment and Data Analysis

A. Animal Preparation

The experimental protocol used in this study has been approved by the Animal Care and Use Committee of Johns Hopkins Medical Institutions. The female Sprague-Dawley (SD) rat (~ 325 g) was anesthetized with intraperitoneal (IP) injection of a mixture of 90 mg/kg of ketamine and 10 mg/kg of xylazine. The rat was constrained in a stereotaxic frame (model 975, Kopf Instruments, Tujunga, CA). A midline incision was made over the scalp and the tissues over the bones were cleaned with a blade. A 6×6 mm2 cranial window overlying the right somato sensory cortex (centered at 4.5 mm lateral and 2.5 mm posterior to the bregma) was thinned with a high speed dental drill (Fine Science Tools, Inc., North Vancouver, Canada) with 1.4 mm steel burr until half transparent. Saline was used to cool down the scalp during the surgery. Rectal temperature was maintained at 37 ◦C throughout the experiment using a Gaymar Heat Therapy System (model TP-500 T/Pump, Gaymar Industries, Inc., New York, NY).

In the brain tumor angiogenesis experiment, the female Fisher 344 rats (~ 170 g) were similarly prepared for imaging. In addition, a 6×6 mm2 cranial window was thinned on the contralateral left cortex (centered at 3.5 mm lateral and 3 mm posterior to the bregma). After recording the baseline raw speckle images on day 0, a hole was drilled carefully at the center of the cranial window with a 1 mm steel burr until the dura was reached.

Then 100 000 cells of 9 L glioma were injected into the cortex using a 26 gauge Hamilton syringe at a depth of 2mmbelow the surface of the cerebral cortex to induce brain tumor. The skin was closed with surgical clips and the rat was housed in the animal facility, as the tumor was allowed to grow.

A 12-bit, cooled CCD camera (Sensicam SVGA, Cooke, MI) with a 60 mm macro (1:1 maximum reproduction ratio) f/2.8 lens was focused on the blood vessels in the cranial window. Exposure time of the CCD was set to 5 ms. Frame rate was 11 ft/s. The imaging field was illuminated with a 632 nm He–Ne Laser beam source (1508P-O, Uniphase, CA). The laser beam was reshaped by a lens to illuminate the entire thinned skull window. The field of view recorded by the CCD camera was 704×704 pixels corresponding to an imaging area of 4.7 × 4.7 mm2 on the rat's brain.

B.Data Recording and Processing

In the SD rat experiment, a white light reflectance image (40-ms exposure time) was obtained first for reference. Following that, a stack of 80 raw speckle images were acquired sequentially.

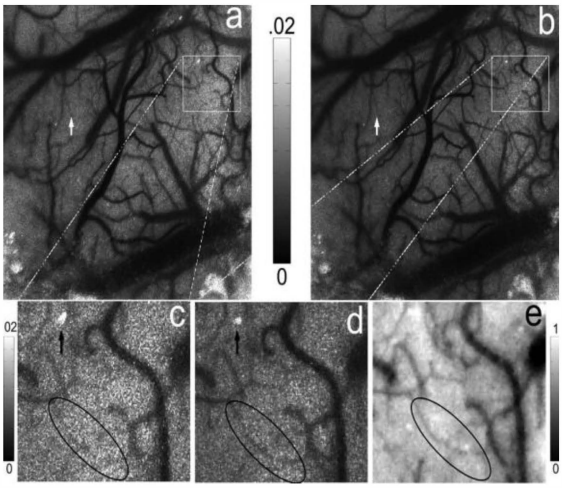

Fig. 4. rLASCA improves the spatial resolution of contrast image. (a) Contrast image based on original unregistered raw speckle images. (b) Contrast image of rLASCA. The white arrows in (a) and (b) indicate the same small vessel which can be seen more clearly in (b) than in (a). (c) and (d) Zoomed out images of the white box area in (a) and (b), respectively. The black arrows in (c) and (d) show the suppression of blur effect. (e) White light image of the corresponding area.

In the brain tumor experiment, the baseline recordings were performed on the day of tumor inoculation (day 0). After that, on day 10, the Fisher rat was imaged again to investigate the angiogenesis. All data were analyzed by both traditional LASCA and rLASCA.

IV. RESULTS

Fig. 3(a) shows an example of the raw speckle images acquired by the camera. Fig. 3(c) zooms out the white box area in Fig. 3(a) with some overexposed pixels in the first ten frames. The disturbances among the images are obvious. After the registration [see Fig. 3(d)], the effect of such disturbances is removed.

A. Revealing Small Vessels Under Higher Resolution

Fig.5., Resulted output of contrast rLASCA

Fig. 5 shows the contrast images based on unregistered (k^2) and registered ($\widehat{k^2}$)raw speckle images, respectively. Although the major vascular structures in k^2 are similar to that in $\widehat{k^2}$, smaller vessels can be recognized more clearly in $\widehat{k^2}$white arrows in Fig. 4 (a) and (b)] after eliminating the disturbances. The over-exposed area (black arrows) in Fig processed by rLASCA is smaller than that in Fig shows it is processed by LASCA, implying that the blur effect is eliminated.

Human vision system produces the most efficient segmentation output which is always used as the gold standard for image segmentations. To obtain the gold standard, ten human observers (all of them are graduate students at Johns Hopkins University with fair understanding of vascular images)were randomly divided into two groups. Fig. 4(c) was presented to the observers in the first group, while observers in the second group were asked to look at Fig. 4(d). All observers needed to judge if there is a vessel in the black circled area. Only one observer in the first group thought there was a vessel within the circle in Fig. 4(c), while the second group unanimously observed a vessel within the same area in Fig. 4(d). This experiment indicated that the small vessel could only be distinguished by rLASCA. Fig. 4(e) shows the white light image of the corresponding area as the ground truth image.

B. Alleviating Noises in Both Tissue and Vessel Areas

The disturbances may result in unreliable contrast values, which could exist in both the tissue and vessel areas. The contrast values are inversely proportional to blood velocity; leading tissue areas always have higher contrast values (smaller velocity) than vessels (arterioles and venules). rLASCA alleviates the noise in the tissue area [e.g., circled area in Fig. 4(b)], while still preserving the distinguishability between tissue and vessel.

. According to the right tail paired *t*-test, the fluctuation level of $k^2$was significantly higher than that of $\widehat{k^2}(p < 0.001)$, which indicating that rLASCA has a better denoising performance in vessel areas.

C. Performance analysis of various LASCA

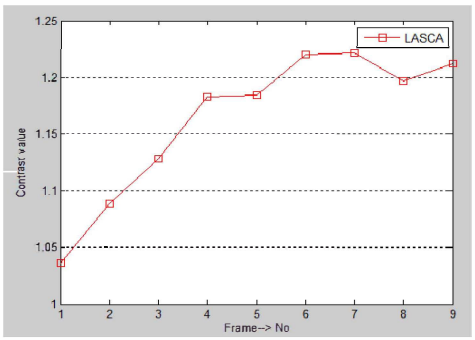

Fig 6: performance of LASCA method

In LASCA method, contrast value increases with respect to its frame change. It seems to be increase in contrast value causes change in image, means not possible to differentiate blood vessels.

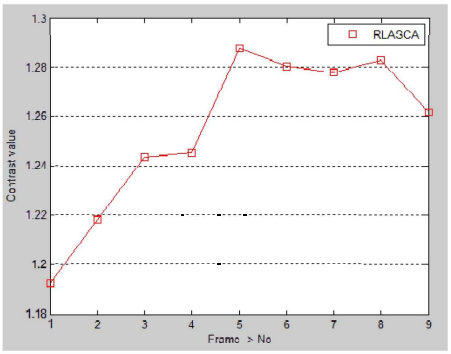

Fig 7: performance of rLASCA method

In rLASCA method, contrast value decreases with respect to its frame change. It shows decrease in contrast value makes the blood flow in blood vessels is visible. Various LASCA methods are under analysis for their performance ratings. Among these performance analysis, rLASCA shows best performance than LASCA.

D. Application in Investigating Brain Tumor Angiogenesis

One of the advantages of rLASCA is to improve the spatial resolution of contrast images of cortical microvasculature. Such a high resolution view is very useful in assessing the changes of cortical vascular. In this study, we applied rLASCA to investigate the angiogenesis of rat's brain tumor. Using rLASCA, microvessels resulting from angiogenesis can be distinguished more clearly from the tissue area. In particular, in some areas, the small vessel and its branches can only be seen by rLASCA.

V. DISCUSSION

A. Sources of Disturbances in LSI

To confirm that the disturbances do originate from respiration and heart beating, we ran similar experiments on hairless mice (strain SKH1). After anesthetizing the mouse, its right ear was rigidly taped onto a glass slide so that there was no effects from respiration and heart beating. Then, the mouse's ear was imaged using the same imaging procedure. Similar to the above procedure, 80 speckle images were recorded and analyzed by both LASCA . All the rigid translation parameters for registration are found to be much closed to zero, indicating no disturbances at all. Comparing k^2 with $\widehat{k^2}$, there were no observable differences between corresponding Fig. which further confirms that the main sources of the image disturbances are respiration and heart beating. This result indicates LASCA and rLASCA produce the same contrast image in the absence of disturbances. However, the source of disturbances is unavoidable in most *in vivo* imaging experiments, and thus need to be suppressed by rLASCA. It should be noted that the periodic noise can also be removed by filtering the images acquired at much higher sampling rate. However, in this study, the disturbances were mainly from respiration and heart beating after a thinned skull preparation. The frequency of noise originating from disturbances is difficult to be estimated in the temporal domain, so the filtering technique is not appropriate in this case. In practice, the disturbances may originate from other sources depending on the experiment conditions. For example, when imaging the rat's CBF with an opened skull preparation, the changing of intracranial pressure may result in greater disturbances; similarly, if the experiment involves electrical stimulation, stimulation artifacts could be another source of disturbances. As a general tool, rLASCA can be directly applied to deal with different disturbances.

B. Influences of Different Interpolators

Interpolation is the key step in the registration of raw speckle images. Based on the registered speckle images, here using different interpolators: 1) nearest neighbour interpolator ; 2) linear interpolator; and 3) cubic B-spline interpolator . Registration with the nearest neighbor interpolator is actually based on the integer part of rigid translation parameters, therefore, disturbances cannot be eliminated efficiently. For linear interpolator, although there is no loss in the rigid translation parameters, the range of contrast values is compressed so that the distinguishability between vessel and tissue is poor. The result of linear interpolation resembles a degenerated case of the result of cubic B-spline interpolation. Compared with the other two interpolators, cubic B-spline interpolator produces more accurate registration while preventing the degeneration of the distinguishability between vessel and tissue.

VI. CONCLUSION

In my paper, i propose rLASCA to eliminate the effect of disturbances due to respiration and heart beating during imaging the rat's CBF. Here i implemented a modified registration technique containing a 3×3 convolution kernel, normalized correlation metric and cubic B-spline interpolator to register the raw speckle images accurately. rLASCA improves the spatial resolution of contrast image and alleviates the noisy effect of disturbances. In the application for investigating angiogenesis of rat's brain tumor, rLASCA shows the small vessels with a higher resolution.

REFERENCES

[1] P.Miao, N.Li, N.V.Thakor, S.Tong," High resolution cerebral blood flow imaging by registered laser speckle contrast analysis" *IEEE Trans Biomed. Eng.,* vol.57, no.5, may 2010

[2] P.Miao, M. Li, H. Fontenelle, A. Bezerianos, Y. Qiu, and S. Tong, "Imaging the cerebral blood flow with enhanced laser speckle contrast analysis (elasca) by monotonic pointransformation," *IEEE Trans. Biomed. Eng.*, vol. 56, no. 4, pp. 1127–1133, Apr. 2009.

[3] P. Thevenaz, T. Blu, and M. Unser, "Interpolation revisited," *IEEE Trans. Med. Imag.*, vol. 19, no. 7, pp. 739–758, Jul. 2000.

[4] J. Briers and S. Webster, "Laser speckle contrast analysis (LASCA): A non scanning, full-field technique for monitoring capillary blood flow," *J. Biomed. Opt.*, vol. 1, no. 2, pp. 174–179, 1996.

[5] M. Li, P. Miao, J. Yu, Y. Qiu, Y. Zhu, and S. Tong, "Influences of hypothermia on the cortical blood supply by laser speckle imagings," *IEEE Trans. Neural Syst. Rehabil. Eng.*, vol. 17, no. 2, pp. 128–134, Apr. 2009.

[6] J. D. Briers and X. W. He, "Laser speckle contrast analysis (LASCA) for blood flow visualization: Improved image processing," *Proc. SPIE*, vol. 3252, pp. 26–33, 1998.

[7] J. Staal, M. Abramoff, M. Niemeijer, M. Viergever, and B. Van Ginneken, "Ridge-based vessel segmentation in color images of the retina," *IEEE Trans. Med. Imag.*, vol. 23, no. 4, pp. 501–509, Apr. 2004.

[8] H. Cheng, Q. Luo, Q. Liu, Q. Lu, H. Gong, and S. Zeng (2004) "Laser speckle imaging of blood flow in microcirculation" *Phys. Med. Biol.*, vol. 49, no. 7, pp. 1347-1357

[9] H. Cheng, Q. Luo, S. Zeng, S. Chen, J. Cen, and H. Gong (2003) "Modified laser speckle imaging method with improved spatial resolution" *J. Biomed. Opt.*, vol. 8, no. 3, pp. 559-564

[10] J. Briers, "Laser Doppler, speckle and related techniques for blood perfusion mapping and imaging," *Physiol. Meas.*, vol. 22, no. 4, pp. 35–66, 2001.

[11] A. Dunn, H. Bolay, M. Moskowitz, and D. Boas, "Dynamic imaging of cerebral blood flow using laser speckle," *J. Cereb. Blood Flow Metab.*, vol. 21, pp. 195–201, 2001.

[12] A. Kharlamov, B. Brown, K. Easley, and S. Jones, "Heterogeneous response of cerebral blood flow to hypotension demonstrated by laser speckle imaging flowmetry in rats," *Neurosci. Lett.*, vol. 368, no. 2, pp. 151–156, 2004.

[13] T.Durduran,M. Burnett, G.Yu, C. Zhou, D. Furuya, A.Yodh, J. Detre, and J. Greenberg, "Spatiotemporal quantification of cerebral blood flow during functional activation in rat somatosensory cortex using laser-speckle flowmetry," *J. Cereb. Blood Flow Metab.*, vol. 24, pp. 518–525, 2004.

[14] D. Zhu, W. Lu, Y.Weng, H. Cui, andQ. Luo, "Monitoring thermal-induced changes in tumor blood flow and micro vessels with laser speckle contrast imaging," *Appl. Opt.*, vol. 46, no. 10, pp. 1911–1917, 2007.

[15] J. Snyman, *Practical Mathematical Optimization: An Introduction to Basic Optimization Theory and Classical and New Gradient-Based Algorithms.* New York: Springer-Verlag, 2005.

[16] J. Parker, R. Kenyon, and D. Troxel, "Comparison of interpolating methods for image resampling," *IEEE Trans. Med. Imag.*, vol. MI-2, no. 1, pp. 31–39, Mar. 1983.

[17] X. W. He and J. D. Briers, "Laser speckle contrast analysis (LASCA): A real-time solution for monitoring capillary blood flow and velocity," *Proc. SPIE*, vol. 3337, pp. 98–107, 1998.

[18] H. Cheng and T. Q. Duong, "Simplified laser-speckle-imaging analysis method and its application to retinal blood flow imaging," *Opt. Lett.*, vol. 32, no. 15, pp. 2188–2190, Aug. 2007.

[19] S. Yuan, A. Devor, D. A. Boas, and A. K. Dunn, "Determination of optimal exposure time for imaging of blood flow changes with laser speckle contrast imaging," *Appl. Opt.*, vol. 44, no. 10, pp. 1823–1830, Apr. 2005.

[20] T. M. Le, J. S. Paul, H. Al-Nashash, A. Tan, A. R. Luft, F. S. Sheu, and S. H. Ong, "New insights into image processing of cortical blood flow monitors using laser speckle imaging," *IEEE Trans. Med. Imag.*, vol. 26, no. 6, pp. 833–842, Jun. 2007.

[21] B. Ruth, "Measuring the steady-state value and the dynamics of the skin blood flow using the non-contact laser speckle method," *Med. Eng. Phys.*, vol. 16, no. 2, pp. 105–111, 1994.

[22] Y. Tamaki, M. Araie, E. Kawamoto, S. Eguchi, and H. Fujii, "Noncontact, two-dimensional measurement of retinal microcirculation using laser speckle phenomenon," *Invest. Ophth. Vis. Sci.*, vol. 35, no. 11, pp. 3825–34, 1994.

[23] A. V¨olker, P. Zakharov, B. Weber, F. Buck, and F. Scheffold, "Laser speckle imaging with an active noise reduction scheme," *Opt. Expr.*, vol. 13, no. 24, pp. 9782–9787, 2005.